Loss of strength in Ni3Al at elevated temperatures

Bernard Viguier, T. Kruml, Jean-Luc Martin

Loss of strength in Ni_3Al at elevated temperatures

B. VIGUIER*†, T. KRUML‡§ and J. L. MARTIN§

†ENSIACET-INP, CIRIMAT, F-31077, Toulouse Cedex 4, France
‡Institute of Physics of Materials, CZ 616 62 Brno, Czech Republic
§IPMC, Swiss Federal Institute of Technology (EPFL), CH-1015 Lausanne, Switzerland

Stress decrease above the stress peak temperature (750 K) is studied in ⟨123⟩ single crystals of Ni_3(Al, 3 at.% Hf). Two thermally activated deformation mechanisms are evidenced on the basis of stress relaxation and strain rate change experiments. From 500 to 1070 K, the continuity of the activation volume/temperature curves reveals a single mechanism of activation enthalpy 3.8 eV/atom and volume $90\,\boldsymbol{b}^3$ at 810 K with an athermal stress of 330 MPa. Over the very same temperature interval, impurity or solute diffusion towards dislocation cores is evidenced through serrated yielding, peculiar shapes of stress–strain curves while changing the rate of straining and stress relaxation experiments. This complicates the identification of the deformation mechanism, which is likely connected with cube glide. From 1070 to 1270 K, the high-temperature mechanism has an activation enthalpy and volume of 4.8 eV/atom and $20\,\boldsymbol{b}^3$, respectively, at 1250 K.

1. Introduction

The strength of Ni_3Al compounds has been extensively studied and modelled in the temperature domain corresponding to the anomalous flow stress behaviour with respect to temperature (for reviews, see [1–3]). However, above the temperature T_p at which stress peaks, data is much less abundant. Early papers report a marked decrease in stress as temperature increases [4], an increase in stress for increasing strain rates [5], or no stress asymmetry in tension and compression tests [6]. Such observations are the signature of thermally activated mechanisms in which the dislocation interaction with stress is less complex than in the stress anomaly domain. Slip-trace analysis and microstructural features in single slip-oriented crystals are also available; this will be discussed further in section 4.3. Therefore, the aim of this study is to contribute to the characterization of the plasticity mechanisms that take over in Ni_3Al above T_p.

The material is presented as follows: firstly, mechanical test data are examined, with emphasis on flow stress as a function of temperature at various strains. Secondly, the strain-rate effect on stress is investigated through stress relaxation and strain-rate change experiments. The activation volume is examined as a function of temperature, stress and strain, so as to determine the domains over which specific

*Corresponding author. Email: bernard.viguier@ensiacet.fr

DOI: 10.1080/14786430500522610

mechanisms operate. Activation energies are also determined. All results are discussed in terms of the possible rate-controlling processes that underlie the loss of strength under the present conditions, taking into account published microstructural observations.

2. Experimental procedures

2.1. *Materials*

⟨123⟩-oriented single crystals were used of composition Ni_3(Al, 3 at.% Hf). Previous studies have been performed on the same crystals, such as the determination of fault energies in dislocation cores [7], the connection between flow stress and dislocation densities [8] or the evaluation of the stress component related to the long-range dislocation interactions through dip tests [9].

2.2. *Mechanical tests*

Specimens ($3.5 \times 3.5 \times 7\,mm^3$) were cut with a diamond saw and mechanically polished. Compression tests were performed on a Schenck RMC 100 machine at a shear strain rate $\dot{\gamma}$ close to $10^{-4}\,s^{-1}$ (unless otherwise specified) between 670 and 1270 K, under a helium atmosphere. τ and γ are, respectively, shear stresses and strains, resolved along the primary octahedral system. $\dot{\gamma}_p$ is the plastic shear strain rate.

Strain-rate change tests, as well as single and repeated stress relaxation experiments [10], were performed. They provide the apparent activation volume V_a, which expresses the stress dependence of the strain rate, as well as the microscopic activation volume, which characterizes the stress dependence of the dislocation velocity [11]. Several such transient tests were performed along monotonic curves, at a strain distance sufficient not to disturb the general shape of the curve.

3. Results

3.1. *Deformation curves*

Typical stress–strain curves exhibit a high work-hardening rate in the preplastic stage, which decreases gradually to a moderate value after the yield stress. Then, it remains approximately constant up to an 18% strain. The general aspect of the curves remains the same for increasing temperatures.

The stress $\tau_{0.2}$, which corresponds to a 0.2% plastic shear strain, is first considered and represented in figure 1a as a function of temperature. Two sets of data points are shown in figure 1a: those that correspond to the present study (670–1270 K), together with earlier data from [12] of between 120 and 800 K. The latter were obtained on crystals cut from the same rod, with the same orientation and deformed at the same strain rate as the present set up. Figure 1a shows that the two sets fit rather well together. Results below confirm this reasonable agreement. As the

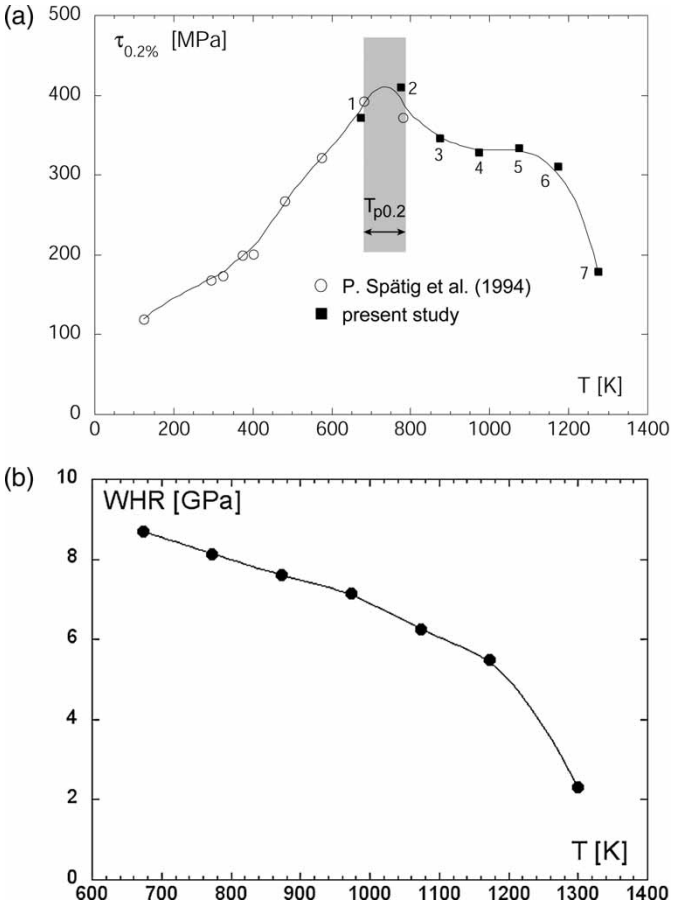

Figure 1. (a) Stress $\tau_{0.2}$ as a function of temperature. $\dot{\gamma} = 10^{-4}\,s^{-1}$. The data-point numbers refer to figure 2. (b) Work-hardening rate (WHR) measured at a plastic strain of 0.2% as a function of temperature.

temperature increases, the stress reaches a maximum for $T_{p0.2}$, with $673\,K < T_{p0.2} < 773\,K$. It then decreases until $T = 1100\,K$. This corresponds to a thermally activated deformation mechanism at intermediate temperatures. At higher temperatures, $\tau_{0.2}$ decreases more steeply with increasing temperature, thus, revealing a transition towards a high temperature mechanism. The work-hardening rate, measured at the same plastic strain, is plotted in figure 1b as a function of temperature. It shows a moderate decrease with temperature up to 1150 K, then a more abrupt decrease. This is thought to correspond to the transition between the intermediate and high temperature mechanisms.

3.2. *Strain-rate dependence on stress*

This dependence can be characterized by the apparent activation volume V_a which is defined by:

$$V_a = kT\left(\frac{\partial \ln \dot{\gamma}}{\partial \tau}\right)_T \tag{1}$$

where k is the Boltzmann constant, T the absolute temperature. The importance of this parameter will be illustrated below. Experimentally, V_a can be determined, provided a change in strain-rate $\Delta \ln \dot{\gamma}$ and the corresponding change in stress $\Delta\tau$, are known from the same experiment. This can be a stress relaxation test, remembering that the stress-rate is proportional to the plastic strain-rate. Therefore, measuring the stress-rate at two points along the relaxation curve allows one to obtain V_a, using relation (1). It can also be determined through a strain-rate jump experiment, in which the strain-rate is suddenly increased and the corresponding change in stress measured. Both methods have been used extensively in the present study.

3.2.1. Stress relaxation tests. The results are presented on figure 2, where V_a is measured at a resolved plastic strain $\gamma_p = 0.2 \times 10^{-2}$. It is first plotted as a function of stress (figure 2a), then of temperature (figure 2b), for stresses below 420 MPa

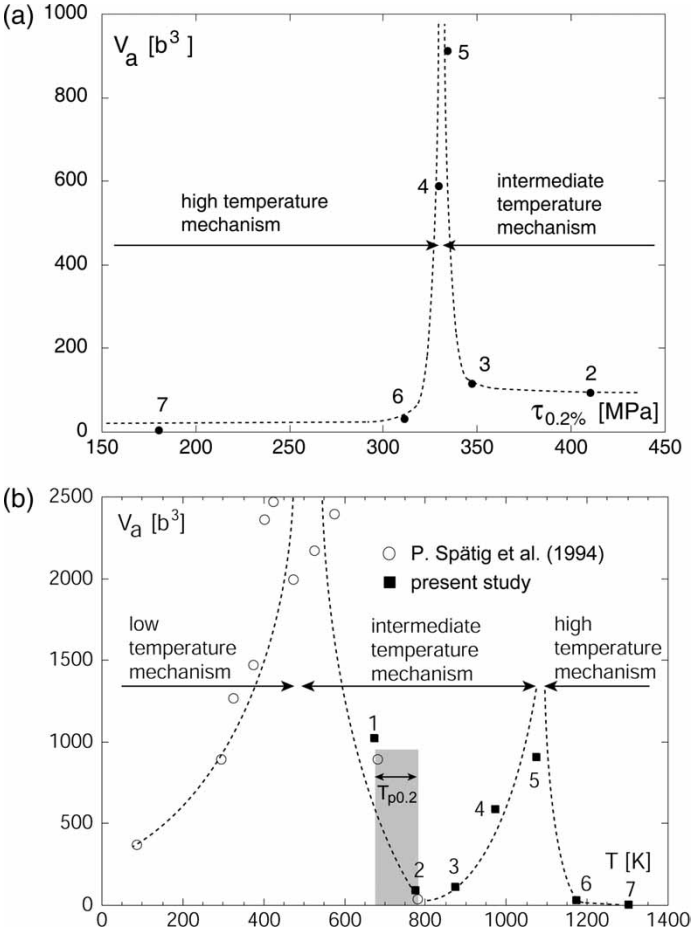

Figure 2. Apparent activation volumes, measured by stress relaxation experiments at $\gamma_p = 0.2 \times 10^{-2}$, (a) as a function of stress and (b) as a function of temperature. Open circles are data by Spätig *et al.* [12]. The data-point numbers are the same as in figure 1 (***b*** is the Burgers vector of the superpartial dislocation).

and temperatures above 700 K. In figure 2b, data by Spätig *et al*. [12] are added for comparison. They refer to lower temperatures compared to the present study, i.e. to the anomalous behaviour of stress with respect to temperature. Figure 2b shows that the two data sets fit satisfactorily together (see V_a values around 680 and 770 K). In addition, they seem to follow the same $V_a(T)$ curve.

Figure 2 exhibits the classical features of the $V(\tau)$ or $V(T)$ curves as different thermally activated mechanisms take over following changes in stress or temperature [13]. More precisely, figure 2 shows that for stresses decreasing from 420 MPa, or temperatures above 750 K (see data points 2 and 3), the volume is approximately constant and close to $90\,\boldsymbol{b}^3$ (where $\boldsymbol{b}$ is the Burgers vector of the superpartial dislocation). This corresponds to the first thermally activated deformation mechanism above T_p, i.e. the intermediate temperature mechanism. Data points 4 and 5 in figure 2 show that, as the stress approaches 330 MPa and the temperature 1070 K, V_a suddenly increases to very high values. This is the signature of a change in dislocation motion mechanism, the intermediate temperature mechanism becoming athermal, with a long-range elastic interaction stress of about 330 MPa and an athermal temperature of 1070 K. This sudden increase in V_a is justified in appendix A. This change was also illustrated in section 3.1, on the curve of figure 1a: it shows that, above 700 K, the stress decreases and reaches a plateau in the vicinity of $\tau = 330$ MPa and $T = 1070$ K. This example illustrates once more that the athermal stress and temperature of a given mechanism are more accurately determined on, respectively, the $V_a(\tau)$ and $V_a(T)$ curves compared to the $\tau(T)$ curves [13].

After this discontinuity of the activation volume, data points 6 and 7 in figure 2 indicate that V_a exhibits a low value, of the order of $20\,\boldsymbol{b}^3$, and is approximately constant from 300 to 170 MPa or 1170 to 1270 K. It corresponds to the high temperature thermally activated mechanism in agreement with the decreasing $\tau(T)$ curve of figure 1, at and above 1150 K (points 6 and 7).

3.2.2. Strain-rate change experiments. To compare the activation volumes measured by stress relaxation and strain-rate change techniques, the latter experiments have been performed at plastic strains of between 10×10^{-2} and 16×10^{-2}, for which the stress jump is more easily measured. The sample response to an increase in strain-rate (by a factor of $\sim$5) depends on temperature: at 1073 K, for instance, the $\tau(\gamma)$ curve exhibits, after the jump, a rounded yield point of moderate amplitude. This can be attributed to the activation of dislocation sources as the strain-rate is suddenly increased. Then, a new steady state is achieved that corresponds to a slightly lower stress. Conversely, at 1173 K, a normal type of response is observed, i.e. the stress increases monotonically following the increase in strain-rate. These two types of transients will be discussed in section 3.3.

The good agreement between V_a values, measured by stress relaxation and strain-rate change techniques, at a plastic strain close to 10×10^{-2}, is illustrated in figure 3 as a function of temperature. V_a values are alike at 873 and 1073 K. In addition, both sets of data seem to follow the same $V_a(T)$ curve.

To better determine the temperature domains associated with given mechanisms, the stress, measured under the same conditions, is also represented in the same figure. At temperatures corresponding to strain-rate jump experiments, the stress, measured at the higher strain-rate, is also plotted in figure 3. This figure shows that the stress corresponding to the lower strain-rate, as well as V_a, exhibit trends as a function

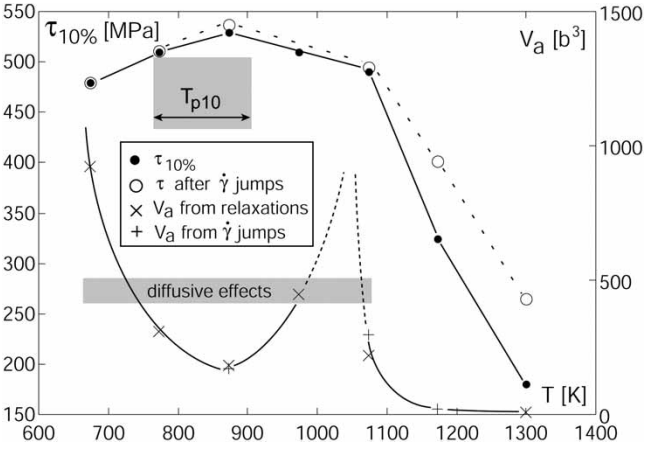

Figure 3. Temperature dependence of the stress and the activation volume, measured at a 10% plastic strain. V_a values are determined by both stress relaxation and strain-rate jump experiments. Stresses correspond both to the nominal strain-rate and to that strain-rate multiplied by 5. The temperature range of diffusive effects is marked by the horizontal bar (see text).

of temperature similar to those at lower strains (see figures 1 and 2b for comparison). At 673 K, $\tau_{10\%}$ increases with temperature and strain-rate insensitive, while V_a decreases. These features are well known for the temperature domain corresponding to the strength anomaly, see, e.g. [12]. Under such conditions, the temperature of maximum stress is T_{p10}, with 780 K < T_{p10} < 900 K, and the stress is slightly strain-rate sensitive at 773 and 873 K. The uncertainty on T_{p10} is related to the shallow maximum of the curve. In particular, it is not possible to say whether T_{p10} is higher or lower than $T_{p0.2}$. Between 873 and 1073 K, the stress decreases and becomes strain-rate-dependent. This corresponds to the intermediate temperature mechanism, with an activation volume smaller than, or of the order of, 200 $\boldsymbol{b}^3$.

Around 1073 K, a marked change in the slope of the $\tau(T)$ curve is observed, while V_a increases towards large values. These features are the signature of a change in mechanism with an athermal temperature of ~1070 K for the intermediate temperature mechanism. The corresponding athermal stress (on the $\tau(T)$ curve) is 490 MPa. Above 1073 K, the high temperature thermally activated mechanism is also observed in figure 3. The stress decreases steeply for increasing temperatures and is strain-rate-dependent. V_a is very low (close to 20 $\boldsymbol{b}^3$) and constant with temperature.

3.3. *Evidence of diffusive effects*

Under adequate temperatures corresponding to slow diffusion, dislocations moving slowly or arrested at obstacles may attract solute atoms or impurities towards their cores. This results in a slowing down or pinning the slow dislocations with no effect on the fast ones. These mechanisms are sometimes reported at specific temperatures in a few of the numerous studies available on the plasticity of Ni_3Al compounds. For example, some of the curves presented by Demura and Hirano [14] show evidence of serrated yielding in single crystals of stoichiometric Ni_3Al between 290 and 530 K for a strain-rate of $8.3 \times 10^{-6}\,s^{-1}$. Similarly, in the early work of

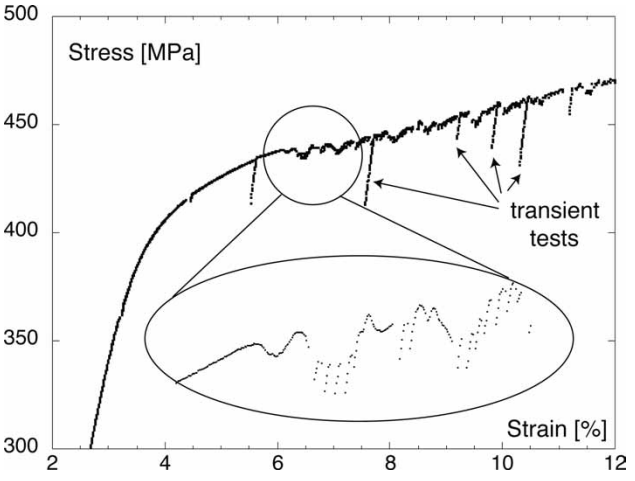

Figure 4. Example of serrated yielding along a stress strain curve at 673 K. An enlargement of the curve is shown in the insert.

Thornton *et al.* [4], a zero or negative strain-rate sensitivity of the stress is measured in similar compounds. Though not much attention is generally paid to these effects, they are likely to influence mechanical behaviour over a temperature range. The conditions for observation of these effects are first listed and then the temperature range over which they take place is determined.

They are thought to account for the two different types of observations during the strain-rate jump experiments of section 3.2.2. At sufficiently high temperatures (e.g. 1173 K), diffusion is sufficiently fast for impurity or solute clouds to move along with dislocations. Imposing a higher straining rate increases the stress regularly so as to increase the dislocation velocity accordingly. At lower temperatures (such as 1073 K), the smooth yield point that follows the jump suggests the following interpretation: at low strain rate, few dislocations are proceeding slowly (impurity or solute pinning), while during the jump, an excess of stress is temporarily required for unpinning to activate dislocation sources and increase their velocity.

Serrated yielding along the stress–strain curves is also observed at intermediate temperatures for plastic strains larger than about 5×10^{-2}. This effect is present with or without performing stress relaxation experiments during straining. An example of serrations is shown in figure 4, at 673 K. It is thought that such behaviour is due to dynamic strain ageing, as in metallic alloys.

A peculiar aspect of some repeated stress relaxation curves, illustrated in figure 5, has also been observed. Usual stress relaxation series exhibit a stress drop for each relaxation, which decreases along the series, at least in the case of hardening [11]. This is also observed here in figure 5. However, the strain-rate at the end of a usual relaxation is commonly found to be smaller than the strain-rate at the onset of the following one. This is because the sample is reloaded after each relaxation, a higher stress inducing a higher deformation rate. In the present case, the table of figure 5 displays these various rates, with the onset rates in the left column. It shows a different trend: the plastic resolved strain-rate $\dot{\gamma}_p$ in (1′) is slightly larger than in (2), larger in (2′) than in (3) and larger in (3′) than in (4). This is opposite to the usual behaviour and reflects a negative strain-rate sensitivity. This can be explained by considering that, during reloading (e.g. between (1′) and (2)),

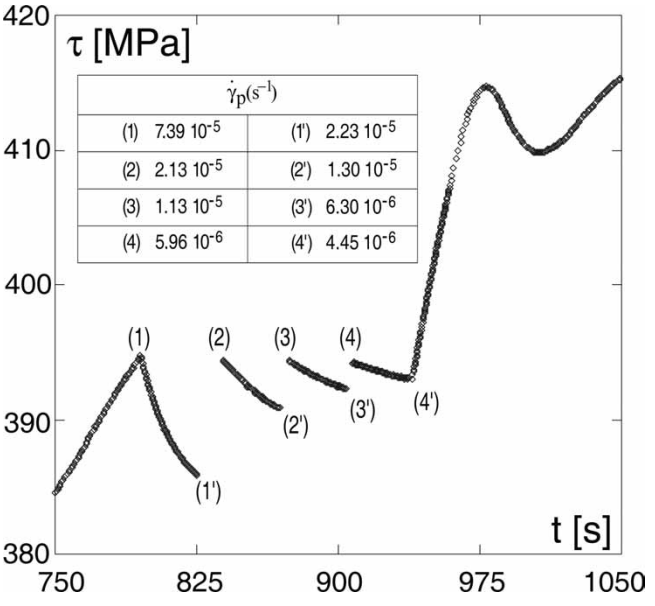

Figure 5. Stress/time curve for a series of four successive relaxations performed along a monotonic curve at 873 K. $\gamma_p = 10^{-2}$. Points (1)–(4) correspond to the onset of each relaxation curve and (1′)–(4′) to the end. Plastic strain-rates measured at these points are displayed in the table. Constant strain-rate is applied before point (1) and after point (4′). Note the yield point at reloading ($t \approx 975$ s).

diffusive effects pin practically immobile dislocations, so that the following relaxation starts with a lower mobile dislocation density. In particular, this effect prevents the determination of the microscopic activation volume, though this is straightforward in the case of conventional relaxation series [15].

Finally, figure 5 shows a yield point during constant strain-rate reloading just after the relaxation series. This feature is again not commonly observed. It is thought to correspond here to excess stress necessary for dislocation multiplication or unpinning, subsequently to dislocation exhaustion during the transient test. The temperature domain where these various effects are observed is also shown in figure 3. They operate essentially from 673 to 1073 K.

The diffusive processes in question can consist of: (i) solute atom or impurity diffusion to the superdislocation core (Cottrell effect), (ii) the relaxation of the atomic structure along the antiphase boundaries (APB) [16] and (iii) the change of APB plane by climb. These three processes similarly affect the dislocation velocity. The present study also shows that they are more marked at larger strains, as more dislocations are involved. They operate at temperatures high enough to cause diffusion over short distances but low enough to prevent fast diffusion.

4. Discussion

4.1. *One or two mechanisms above* T_p*?*

In sections 3.1 and 3.2, the temperature (and stress) domains that correspond to two thermally activated mechanisms have been evidenced above T_p considering both

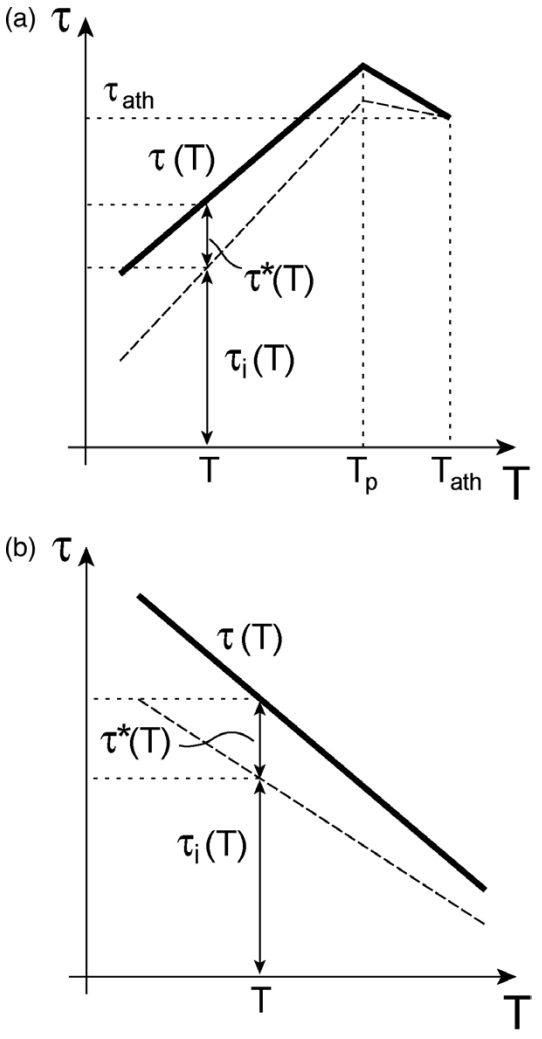

Figure 6. Schematic representation of the temperature dependence of τ, τ^* and τ_i for (a) the upper end of the intermediate T domain and (b) the high-temperature mechanism.

the changes in slope of the $\tau(\gamma)$ curves and the discontinuities of V_a. These two mechanisms are now critically examined in light of the present data, as well as earlier results.

Among the few available studies of Ni_3Al compounds above T_p, Heredia and Pope [17, 18] report only one monotonic decrease of stress for temperatures rising above T_p. In these two papers, single crystals of binary Ni_3Al and ternary compounds, containing from 0.2 to 1 at.% B or 1 to 3.3 at.% Hf or 1 and 2.5 at.% Ta, were deformed in air at a rate of $10^{-3}\,s^{-1}$ up to 1350 K. Conversely, in a deformation study of Ni_3(Al, 1 at.% Ta) single crystals in the ⟨123⟩ orientation, Baluc *et al.* [19, 20] report $\tau_{0.2}(T)$ curves quite similar to those of figure 1: above T_p, they exhibit two temperature domains with different rates of stress decrease with temperature. Moreover, as the strain rate is changed from $7 \times 10^{-5}\,s^{-1}$ to $7 \times 10^{-4}\,s^{-1}$, the stress is observed to increase in both temperature domains [19], similar

to figure 3. The difference between the two types of data sets can be explained if one compares the experimental procedures in the two studies. The former authors deform successively the same sample up to a 0.2% strain at each investigated temperature. Conversely, in the present study and in [19], a new sample is tested at each temperature. It has been shown by Spätig *et al*. [12] that only the latter procedure is reliable. Therefore the existence of two successive thermally activated processes operating above T_p seems to be established for Hf- and Ta-containing compounds.

4.2. *Activation energies*

The identification of both mechanisms is extended, considering activation energy values and available substructure data.

Activation enthalpy values can be obtained from the present results using the relation:

$$\Delta H = -TV_a\left(\frac{d\tau}{dT}\right)_{\dot{\gamma}} \tag{2}$$

Determination of ΔH has been attempted at temperatures corresponding to minima in the $V_a(T)$ curves, i.e. as far as possible from the athermal conditions and at a plastic strain of 0.2%, where data are more accurate (figure 1 and 2b). ΔH is found to be close to 3.8 eV/atom at 810 K (intermediate temperature mechanism) and 4.8 eV/atom at 1250 K (high temperature mechanism). It is worth noting that these results differ from those of a preliminary study [21] due to the more accurately determined V_a values in the present work.

4.3. *Rate controlling mechanisms*

Table 1 summarizes the characteristics of the deformation mechanisms identified in the present study.

The continuity of the $V(T)$ curve, illustrated in figures 2 and 3, suggests unambiguously that a single intermediate temperature mechanism operates from 500 to 1050 K (for $\gamma_p = 0.2 \times 10^{-2}$), i.e. below and above T_p, respectively. The corresponding activation energy is 3.8 eV/atom and, at temperatures T_{ath} close to 1050 K, it becomes athermal and the stress value τ_{ath} of about 340 MPa represents the long-range elastic interaction of the mobile dislocations with the substructure.

For intermediate temperature conditions around T_p, transmission electron microscope observations and slip-line studies reveal dislocations gliding on the

Table 1. Characteristics of intermediate (T_{int}) and high (HT) temperature mechanisms.

γ_p		T_{int}	HT
0.2%	τ_{ath}	330 MPa	<170 MPa
	T_{ath}	1070 K	<1270 K
	V_{amin}	$90\,\boldsymbol{b}^3$	$\leq 20\,\boldsymbol{b}^3$
	ΔH	3.8 eV/atom	4.8 eV/atom
$\cong 10\%$	τ_{ath}	490 MPa	<180 MPa
	T_{ath}	1050 K	>1270 K
	V_{amin}	$\leq 200\,\boldsymbol{b}^3$	$\cong 10\,\boldsymbol{b}^3$

cube planes (see e.g. [1, 22] for the present samples, and the in situ experiments on Ni_3(Al, 0.25 at.% Hf) in [23]). These observations reveal friction forces acting on both screws and edges, due to their core being sessile with respect to cube glide. It is also remarkable that the temperature range where diffusive effects operate coincides with that of the intermediate temperature mechanism (figure 3). Several intimations as to the operation of such processes have appeared throughout this study in the various experiments performed. They consist successively in the peculiar aspect of the $\tau(\gamma)$ curve after a strain-rate change (section 3.3.2.), the occurrence of serrated yielding on the monotonic curves with or without transient tests (figure 4), of a yield point of small amplitude at the onset of reloading after a repeated stress relaxation experiment (figure 5), or the unusual behaviour of stress relaxation curves (figure 5) depending on the conditions. The present observation of the intermediate temperature interval that includes T_p is quite remarkable. It implies that the same mechanism, which is thermally activated, operates over the stress peak and below it, at least under relaxation conditions. Assuming the classical decomposition of the applied stress ($\tau = \tau^* + \tau_i$ – see equation (A3) in appendix A), the present results indicate that the stress anomaly would be related to the behaviour of the athermal part of stress τ_i. Figure 6 illustrates the corresponding variations of τ, τ^* and τ_i for the intermediate and high temperature mechanisms. This constitutes a milestone in the study of the role of thermal activation in the deformation of Ni_3Al, which began more than 15 years ago (see [24] and e.g. [3]).

At higher temperatures, as the diffusive processes mentioned above do not further impede dislocation motion; from about 1070 K, the mechanism that takes over has an activation enthalpy of 4.8 eV/atom, an activation volume smaller than or equal to $20\,\boldsymbol{b}^3$ and does not become athermal before 1300 K, the maximum temperature examined. Some TEM observations report 'exotic' dislocation configurations [25] consisting of (i) two superpartials, each being extended outside the cube plane, or (ii) a split configuration along a dihedron. ⟨100⟩ dislocations have also been seen in Ni_3Al(1 at.% Ta) at 1272 K [26, 27].

It is worth noting that two mechanisms have also been mentioned on the basis of creep experiments [28] in a Ni_3(Al, Hf, B) compound. The intermediate mechanism is observed between 903 and 923 K, with no activation energy reported. At 1273 K, a second mechanism takes over, with an activation energy of 4.96 ± 0.56 eV/atom, which the authors identify as dislocation climb on the basis of diffusion data. It is clear that TEM observations are requested on the samples deformed in the high temperature domain to identify more precisely the operative dislocation mechanism.

5. Conclusions

In Ni_3(Al, 3 at.% Hf) single crystals, the loss of strength above the stress peak temperature is due to the thermal activation of two different processes. This is clearly established in the present compound, as well as in Ni_3(Al, 1 at.% Ta), both in the ⟨123⟩ orientation, on the basis of the variation with temperature of the stress and activation volume.

Between 550 and 1070 K for $\gamma_p = 0.2 \times 10^{-2}$ ($T_p \sim 750$ K), a single intermediate temperature mechanism is evidenced with an activation volume and enthalpy of,

respectively, $90\,\boldsymbol{b}^3$ and 3.8 eV/atom at 810 K. It appears to be connected with cube glide and operates exactly over the domain where diffusive processes are evidenced through various types of experiments. This complicates further identification of the rate-controlling process, which becomes athermal at 1070 K, with an internal stress of 330 MPa. Between 750 K and T_p, under relaxation conditions, dislocation segments proceed under the same intermediate temperature mechanism than slightly above T_p. This observation sheds new light on the upper end of the stress anomaly domain.

From 1070 to 1270 K, a high-temperature mechanism takes over, with an activation volume smaller than or equal to $20\,\boldsymbol{b}^3$ and an activation enthalpy of 4.8 eV/atom at 1250 K. Its complete identification requires further studies, particularly TEM observations of dislocation structures.

The results of these intermediate- and high-temperature mechanisms will stimulate further research on diffusive processes (activation energies, diffusing species) and on high-temperature cube glide mechanisms.

Acknowledgements

The authors would like to express their gratitude to Fonds National Suisse for supporting this research. BV thanks EPFL for leave-of-absence to perform this research in Lausanne.

Appendix A

Since the early days of mechanical testing, the large increase in activation volume, as a deformation mechanism becomes athermal, has been experimentally evidenced. This has been observed in a number of crystals deforming under conventional thermally activated processes and for various deformation conditions (constant strain rate, creep). Examples can be found in [29] and [30] for Ti, in [31] for Zr, and in [32] for Mg. However, to the best of our knowledge, an interpretation of this behaviour has never been proposed. In the following, a brief explanation is developed.

The plastic strain rate is expressed via the Orowan relation:

$$\dot{\gamma}_p = \rho_m \boldsymbol{b} v \tag{A1}$$

where ρ_m is the mobile dislocation density, $\boldsymbol{b}$ their Burgers vector and v their average velocity.

The velocity v obeys thermal activation and depends on stress and temperature via:

$$v = v_0 \exp(-Q/kT)\mathrm{sh}(\tau^* V/kT) \tag{A2}$$

where Q and V are, respectively, the activation energy and volume of the velocity, and τ^* is the effective stress defined by:

$$\tau^* = \tau - \tau_i \tag{A3}$$

where τ_i is the long-range elastic interaction stress. In relation (A2), the hyperbolic sine function, contrary to the more commonly used exponential function, takes into

account the dislocation jumps in the direction opposite to the applied stress. These are especially important as the mechanism becomes athermal (weak τ^* values). Under the latter conditions, $\mathrm{sh}(\tau^* V/kT)$ becomes equivalent to $\tau^* V/kT$ so that according to equations (A1) and (A2), $\dot{\gamma}_p$ is proportional to τ^*. Referring to (1), V_a reaches very high values. The value of τ_i corresponding to the vanishing τ^* is called τ_{ath} in the text.

References

[1] P. Veyssière and G. Saada, in *Dislocations in Solids*, edited by F.R.N. Nabarro and M.S. Duesbery, Vol. 10 (Elsevier, Amsterdam, 1996).
[2] D. Caillard and A. Couret, in *Dislocations in Solids*, edited by F.R.N. Nabarro and M.S. Duesbery, Vol. 10 (Elsevier, Amsterdam, 1996).
[3] B. Viguier, J.-L. Martin and J. Bonneville, in *Dislocations in Solids*, edited by F.R.N. Nabarro and M.S. Duesbery (Elsevier, Amsterdam, 2002).
[4] P.H. Thornton, R.G. Davies and T.L. Johnston, Metall. Trans. **1** 207 (1970).
[5] S. Miura, S. Ochiai, S. Oya, *et al.*, in *High Temperature Ordered Alloys III*, edited by C.T. Liu, A.I. Taub, N.S. Stoloff, *et al.* (Material Research Society, Pittsburg, 1989).
[6] Y. Umakoshi, D.P. Pope and V. Vitek, Acta Metall. **32** 449 (1984).
[7] T. Kruml, J.L. Martin and J. Bonneville, Phil. Mag. A **80** 1545 (2000).
[8] T. Kruml, V. Paidar and J.L. Martin, Intermetallics **8** 729 (2000).
[9] T. Kruml and J.-L. Martin, Mater. Sci. Forum **426/432** 1861 (2003).
[10] J.L. Martin, B. Matterstock and P. Spätig, *et al.*, in *20th Riso International Symposium on Material Science* (Riso National Laboratory, Roskilde, 1999).
[11] J.L. Martin, B. Lo Piccolo, T. Kruml, *et al.*, Mater. Sci. Eng. A **322** 118 (2002).
[12] P. Spätig, J. Bonneville and J.L. Martin, in *Strength of Materials*, edited by H. Oikawa, K. Maruyama, S. Takeuchi, *et al.* (Japan Institute of Metals, Tokyo, 1994).
[13] D. Caillard and J.L. Martin, in *Thermally Activated Mechanisms in Crystal Plasticity*, Pergamon Materials Series, edited by R.W. Cahn, Vol. 8 (Elsevier, Oxford, 2003).
[14] M. Demura and T. Hirano, Phil. Mag. Lett. **75** 143 (1997).
[15] J.L. Martin and T. Kruml, J. Alloys Comp. **378** 2 (2004).
[16] N. Brown, Phil. Mag. Lett. **4** 693 (1959).
[17] F. Heredia and D.P. Pope, *High-Temperature Ordered Intermetallic Alloys II* (Materials Research Society, Boston, MA, 1987).
[18] F.E. Heredia and D.P. Pope, J. Phys. III **1** 1055 (1991).
[19] N. Baluc, J. Bonneville and J.L. Martin, Phys. Scripta **T49** 393 (1993).
[20] N. Baluc and R. Schäublin, Phil. Mag. A **74** 113 (1996).
[21] B. Viguier, T. Kruml and J.L. Martin, Mater. Sci. Eng. A **389** 960 (2004).
[22] T. Kruml, J.L. Martin, B. Viguier, *et al.*, Mater. Sci. Eng. A **239** 174 (1997).
[23] G. Molénat and D. Caillard, Phil. Mag. A **65** 1327 (1992).
[24] N. Baluc, J. Stoïber, J. Bonneville, *et al.*, Israel. J. Technol. **24** 269 (1988).
[25] Y.Q. Sun, P.M. Hazzeldine, M.A. Crimp, *et al.*, Phil. Mag. A **64** 311 (1991).
[26] N. Baluc, in *Electron Microscopy*, edited by L.D. Peachey and D.B. Williams (San Francisco Press, San Francisco, 1990).
[27] G. Eggeler and A. Dlouhy, Acta Mater. **45** 4251 (1997).
[28] K.J. Hemker and W.D. Nix, in *Structural Intermetallics*, edited by M.V. Nathal, R. Darolia, C.T. Liu, *et al.* (Minerals, Metals and Materials Society, USA, 1997).
[29] E.D. Levine, Trans. Metall. Soc. AIME **236** 1558 (1966).
[30] M.P. Biget and G. Saada, Phil. Mag. A **59** 747 (1989).
[31] P. Soo and T. Higgings, Acta Metall. **16** 177 (1968).
[32] A. Ahmadieh, J. Mitchell and J. E. Dorn, Trans. Metall. Soc. AIME **233** 1130 (1965).